Acta Crystallographica Section D
Biological Crystallography
ISSN 0907-4449

Structure of human carbonmonoxyhemoglobin at 2.16 Å: a snapshot of the allosteric transition

Martin K. Safo,* James C. Burnett, Faik N. Musayev, Samuel Nokuri and Donald J. Abraham

School of Pharmacy, Department of Medicinal Chemistry and Institute for Structural Biology and Drug Discovery, Virginia Commonwealth University, Richmond, VA 23219, USA

Correspondence e-mail: msafo@hsc.vcu.edu.

Received 24 April 2002
Accepted 3 September 2002

PDB Reference: COHbA, 1ljw, r1ljwsf.

A 2.16 Å resolution structure of high-salt human carbonmonoxyhemoglobin crystallized at pH 6.4 is reported. The quaternary structure is similar to that of 'classic' R-state hemoglobin; however, subtle but significant tertiary structural changes are observed at the $\alpha_1\beta_2$ and symmetrically equivalent $\alpha_2\beta_1$ interfaces – these are the key subunit interfaces that govern the allosteric transition between the R and T states. Specifically, the movement and weakening of two important hydrogen bonds that are diagnostic for R-state structures, β_2His97–α_1Thr38 and β_2Arg40–α_1Thr41, have been observed. In addition, a phosphate molecule bound between the two β-subunits (at the entrance to the central water cavity) has been identified and electron density indicates that this molecule occupies two alternate positions that are related by the dyad axis. Both positions superimpose on the 2,3-diphosphoglycerate binding site. One phosphate conformer interacts with β_2Asn139, β_1His143 and β_1His146, while the second interacts with symmetry-related counterparts (β_1Asn139, β_2His143 and β_2His146).

1. Introduction

Hemoglobin (Hb) is an allosteric tetrameric protein that exists in equilibrium between two alternative structures, the T (tense) state, which possesses low oxygen affinity, and the R (relaxed) state, which has a high oxygen affinity. Perutz (1970, 1972) and Baldwin & Chothia (1979) were the first researchers to elucidate, at atomic resolution, the structures of the classic T and R states of Hb that were used to develop the two-state MWC model of allostery (Monod *et al.*, 1965). Subsequently, a number of high-resolution three-dimensional structures of both the T and R states of Hb from a variety of different species have been reported. The basic tertiary and quaternary structures observed for the T state are all similar, as are those observed for the classic R state (Ladner *et al.*, 1977; Baldwin & Chothia, 1979; Shaanan, 1983, Katz *et al.*, 1994; Vasquez *et al.*, 1998; Safo & Abraham, 2001). Based on these structures, it is clear that the allosteric transition from the T to the R state involves a rotation and a shift of one $\alpha\beta$ dimer relative to the other symmetry-related $\alpha\beta$ dimer. This movement results in a larger central water cavity in the T state and a narrower cavity in the R state. Exclusive binding of 2,3-diphosphoglycerate (2,3-DPG) at the entrance of the larger β cleft of the central water cavity in the T state leads to stabilization of this allosteric form relative to the R state. The additional 2,3-DPG stabilization further decreases the affinity of T-state Hb for oxygen.

Analysis of the quaternary structures of the T and R states of Hb reveal differences in intersubunit contacts that can be

used to characterize these two states. For example, in the T state, β_2His97 from the *FG* corner is positioned between the *C*-helix residues α_1Pro44 and α_1Thr41. Transition to the R state results in the movement of β_2His97 such that it lies between residues α_1Thr41 and α_1Thr38 and engages in a hydrogen-bond interaction with α_1Thr38, as found in human oxygenated Hb (Shaanan, 1983) and human carbonmonoxy Hbs (Baldwin & Chothia, 1979; Vasquez *et al.*, 1998), or with α_1Thr41, as found in pig methemoglobin (Katz *et al.*, 1994). This interaction also occurs in both the R-state structures of horse methemoglobin (Ladner *et al.*, 1977) and bovine carbonmonoxy Hb (Safo & Abraham, 2001). However, structural analyses indicate that this hydrogen bond is significantly weaker in these two structures.

The MWC model for allostery does not include stable intermediate states during the transition from the T to the R state and *vice versa*. However, another liganded Hb structure referred to as R2 (Silva *et al.*, 1992) or Y (Smith *et al.*, 1991; Smith & Simmons, 1994) has been proposed to represent an intermediate between the T and R states (Silva *et al.*, 1992; Smith *et al.*, 1991; Smith & Simmons, 1994). In the R2 state, β_2His97 is also located between α_1Thr41 and α_1Thr38, but does not engage in a hydrogen-bonding interaction with either of these two residues. Srinivasan & Rose (1994) and Schumacher *et al.* (1997) have suggested that the R2 (or Y) structure may correspond to the physiologically relevant end-state of oxygenated Hb and that the classical R-state structure is actually an intermediate trapped between the R2 and T states. However, other investigators have argued that the R2 structure is simply an additional relaxed end-state and not an intermediate in the T to R transition (Janin & Wodak, 1993; Doyle *et al.*, 1992).

This study reports an interesting new R-state human carbonmonoxy Hb structure (COHbA) solved at a resolution of 2.16 Å. The crystals were obtained under high-salt conditions, but at a lower pH (6.4) than the standard growth conditions (pH 6.7) described by Perutz (1968). The quaternary structure of the reported COHbA is indistinguishable from those of other R-state human Hb structures (Baldwin & Chothia, 1979; Shaanan, 1983; Vasquez *et al.*, 1998); however, analyses of intersubunit interactions indicated that there are several key tertiary structural differences. The most striking difference is the loss of the diagnostic R-state hydrogen bond between β_2His97 O and α_1Thr38 OG1, which is replaced by water-mediated hydrogen bonds between α_1Thr38 OG1 and the two residues β_2Asp99 OD1 and α_1Asn97 ND2. Another diagnostic hydrogen-bond pair, β_2Arg40 NH1–α_1Thr41 O, is also unique to the R state. The latter appears to be weakened in the new R-state COHbA structure. In addition, the reported COHbA reveals that a phosphate molecule is bound at the β-subunit C-terminus of the central water cavity, at the exact position occupied by 2,3-DPG in T-state Hb. The phosphate is disordered in two positions that alternate between two sides of the 2,3-DPG binding site and are related by the twofold axis; one phosphate conformer interacts with β-subunit residues β_2Asn139, β_1His143 and β_1His146, while the other interacts with residues β_1Asn139, β_2His143 and β_2His146 of the second β-subunit. Several of these same residues have been shown to engage in contacts with 2,3-DPG in the T state.

Table 1
Crystal information, data collection and refinement parameters for COHbA.

Values in parentheses refer to the outermost resolution bin.

Data-collection statistics	
Space group	$P4_12_12$
Unit-cell parameters (Å)	a = 53.57, b = 53.57, c = 192.95
Molecules per asymmetric unit	1 dimer
Resolution (Å)	2.16 (2.26–2.16)
No. of measurements	44267 (2856)
No. of unique reflections	14441 (1229)
$I/\sigma(I)$	17.3 (5.1)
Completeness (%)	90.2 (62.6)
$R_{\rm merge}$† (%)	5.2 (17.7)
Structure refinement	
Resolution limit (Å)	60–2.16 (2.22–2.16)
σ cutoff (F)	0.0
No. of reflections	14441 (679)
Completeness (%)	100
R factor (%)	19.4 (23.5)
$R_{\rm free}$‡ (%)	25.9 (34.5)
R.m.s.d.s from standard geometry	
Bond lengths (Å)	0.013
Bond angles (°)	1.9
Positional error (σ)	
R factor	0.18
$R_{\rm free}$	0.24
Dihedral angles	
Most favored regions	92.7
Additional allowed regions	7.3
Average B values (Å^2)	
All non-H atoms	34.2
Protein atoms	33.3
Heme atoms	27.6
CO atoms	18.1
Water atoms	44.0
Phosphate	58.9

† $R_{\rm merge} = \sum(\langle I\rangle - I)/\sum I$. ‡ The 5% of the reflections which were used for the calculation of $R_{\rm free}$ were excluded from the refinement.

The results from these analyses raise an interesting question: are the hydrogen bonds that are observed at the $\alpha_1\beta_2$ ($\alpha_2\beta_1$) interface of the classical R-state structure, but are not observed in the reported COHbA structure, really diagnostic of the R state? Or is the COHbA structure reported here a new distinct structure that shows a subtle but significant gradation in the allosteric transition between the R and T states? Based on our observations, we have concluded that the new COHbA is a snapshot revealing the initial intersubunit contact strain that results in the transition from the R- to the T-state structure and that the binding of the phosphate between the two β-subunits is diagnostic of an intermediate structure in which the affinity for 2,3-DPG binding is increased over that of the classical R-state structure.

2. Materials and methods

2.1. Crystallization, X-ray data collection and processing

The crystallization protocol followed that of Perutz (1968) with some slight modifications. The oxygenated Hb solution was evacuated for about 10 min and the resulting deoxy-

genated Hb solution was further reduced by the addition of a small pellet of $Na_2S_2O_4$. The fully reduced deoxygenated Hb solution was then saturated with CO to generate the CO-bound Hb form. Crystallization was carried out with a solution of 40 mg ml^{-1} protein, 3.4 *M* sodium/potassium phosphate pH 6.4 using 7 ml Vacutainer tubes. Two drops of toluene were added to the Hb solution in each tube. More CO was then bubbled into the tubes and the tubes were sealed. Crystals appeared after 4–6 d in several of the tubes containing 2.35–2.65 *M* phosphate. A diffraction data set was collected at 100 K using a Molecular Structure Corporation (MSC) X-Stream Cryogenic Crystal Cooler System (MSC, The Woodlands, Texas, USA), an R-AXIS II image-plate detector equipped with OSMIC confocal mirrors and a Rigaku RU-200 X-ray generator operating at 50 kV and 100 mA. Prior to use in X-ray diffraction, the crystal was washed in a cryoprotectant solution containing 50 µl mother liquor and 12 µl glycerol. The data set was processed with the *MSC BIOTEX* software program. Data-collection and processing statistics are summarized in Table 1.

2.2. Structure determination and refinement

The isomorphous 2.7 Å native human carbonmonoxyhemoglobin structure (PDB code 2hco; Baldwin & Chothia, 1979) was used as the starting model for the refinement of the COHbA structure. The refinement was performed with the *CNS* program (Brünger *et al.*, 1998), with a bulk-solvent correction applied. A statistically random selection of about 5% of the total reflection data was excluded from the refinement and used to calculate the free *R* factor ($R_{\rm free}$) as a monitor of model bias (Brünger, 1992). The model was subjected to rigid-body refinement, with the two Hb subunits treated as independent groups, using data to 2.16 Å. The initial *R* factor dropped from 34.9 to 33.2% with an $R_{\rm free}$ of 30.5%. The model was subjected to one run of positional refinement and simulated annealing. The resulting electron-density maps allowed the fitting of two CO molecules bound to the two heme irons and a phosphate molecule close to the twofold axis at the C-terminus of the β-subunit. Three alternate rounds of positional refinement, simulated-annealing refinement, addition of water and individual *B*-factor refinements with intermittent manual model corrections brought the final *R* factor to 19.4% and the $R_{\rm free}$ to 25.9%. Two residues, αHis89 and βArg40, were refined in two alternate conformations. Model building and correction were carried out using the program *TOM* (Cambillau & Horjales, 1987). The model was also subjected to quality analysis during the various refinement stages with omit maps and the *PROCHECK* program (Laskowski *et al.*, 1993). Refinement statistics are summarized in Table 1.

3. Results

3.1. Crystallographic refinement and structure of COHbA

COHbA crystallized isomorphously with R-state human liganded Hb crystals (PDB code 2hco; Baldwin & Chothia, 1979; PDB code 1hh0; Shaanan, 1983; PDB code 1aj9; Vasquez *et al.*, 1998), which are also obtained from similar high-salt conditions. The final structure contains a dimer ($\alpha_1\beta_1$) in the asymmetric unit and is composed of 141 residues in the α-subunit, 146 residues in the β-subunit, two heme groups, two CO ligands, a phosphate molecule and 261 water molecules. The electron-density map ($2F_o - F_c$) at 1.0σ showed well defined density for the main-chain atoms of the entire polypeptide, except for weak density at the side chain of the C-terminal residue αArg141. Table 1 gives detailed crystallographic statistics.

3.2. Structural comparison with other R-state Hb structures

The high-salt R-state 1aj9 structure, determined at 2.2 Å resolution by Vasquez *et al.* (1998), was used for comparison with the reported COHbA structure, as it has been refined to a higher resolution than any other R-state human carbonmonoxy Hb structure reported to date. The overall dimer ($\alpha_1\beta_1$) and tetramer ($\alpha_1\beta_1 + \alpha_2\beta_2$) conformations for the reported structure compared with those of the R-state structure 1aj9 (by superimposing the C^α atoms of all residues with the exception of three residues from the N- and C-termini of the subunits in each structure) revealed a high degree of similarity, as indicated by the root-mean-square deviations (r.m.s.d.s) of 0.36 and 0.40 Å, respectively. However, there were several notable differences between the two structures. A key diagnostic interaction observed between β_2His97 O and α_1Thr38 OG1 at the $\alpha_1\beta_2$ ($\alpha_2\beta_1$) interface in R-state human Hb structures (Baldwin & Chothia, 1979; Shaanan, 1983; Vasquez *et al.*, 1998) is not observed in the COHbA structure, even though the β_2His97 side chain remains packed between residues α_1Thr41 and α_1Thr38 (Fig. 1*a*). The absence of this hydrogen bond in the COHbA structure results from a new orientation of the α_1Thr38 side chain, which has reoriented (relative to this residue in the classical R-state structure) to engage in water-mediated hydrogen bonds with β_2Asp99 OD1 and α_1Asn97 ND2. This water is absent in 1aj9 (Vasquez *et al.*, 1998), as well as in the 2.1 Å oxyhemoglobin structure 1hh0 (Shaanan, 1983). In addition, it is important to note that the side chain of α_1Thr38 is well ordered and occupies well defined electron density. Omit maps were used to ascertain the correct orientation of the side chain; moreover, reorienting the side chain to allow a hydrogen bond with β_2His97 O resulted in difference negative and positive peaks around the side chain.

Another diagnostic R-state hydrogen bond between β_2Arg40 and α_1Thr41 is only partially present in the COHbA structure. The side chain of β_2Arg40 was highly disordered and occupied many positions, but was defined in two conformations during the refinement. One of the conformers, referred to as conformer 1, displayed 45% occupancy and was very similar to the side-chain position of β_2Arg40 as seen in 1aj9; however, the hydrogen bond between β_2Arg40 NH1 and α_1Thr41 O, which is present in 1aj9 as well as in other R-state Hbs, was abolished. Instead, conformer 1 had moved slightly to engage in a unique water-mediated hydrogen bond with α_1Leu91 O. This water molecule is absent in both 1aj9 and

1hh0. The second conformer (conformer 2) displayed an occupancy of 25% and its unique position allowed a direct 2.6 Å hydrogen-bonding interaction between its guanidinium side-chain moiety and the hydroxyl group of α_1Thr41. Fig. 1(*a*) is the $\alpha_1\beta_2$ interface of COHbA showing the interactions described above. The two contrasting $\alpha_1\beta_2$ interfaces in COHbA and 1aj9 are superimposed and depicted in Fig. 1(*b*).

A striking difference between COHbA and 1aj9 involves interactions associated with the C-terminal residues at the $\beta_1\beta_2$ subunit interface. Analysis of COHbA indicated a large positive tetrahedrally shaped electron density lying between the well defined βHis143 residues and the crystallographic twofold axis at the entrance to the central water cavity (this density is not observed in the high-salt R-state structure 1aj9). A phosphate molecule was fitted to this density (Fig. 2 displays a $2F_o - F_c$ electron-density map calculated around the crystallographic phosphate-molecule binding site). The phosphate molecule and its resulting symmetry-related counterpart lie in close proximity, with a contact distance of only 2.5 Å. However, as the pH of crystallization was 6.4, it is expected that the phosphate molecule is ionized, making it impossible for two unique phosphates to reside in such close proximity. Therefore, it is hypothesized that the observed phosphate densities are actually one molecule that is disordered in two different positions in the Hb tetramer. The two different phosphate conformers sit almost in between the two βHis143 residues; one conformer engages in hydrogen-bonding interactions of distance 3.4, 2.4 and 2.6 Å with residues β_2Asn139, β_1His143 and β_1His146, respectively, while the other conformer engages in symmetry-related interactions with residues β_1Asn139, β_2His143 and β_2His146 (Fig. 3*a*). In addition, a pair of symmetry-related water molecules lying further up the entrance to the central water cavity mediate hydrogen-bonding interactions between the phosphate conformers and βLys82 (Fig. 3*a*). In contrast, the imidazole ring of β_1His143 in 1aj9 engages in a direct side-to-face π interaction with the imidazole ring of β_1His146 (β_2His146) and also engages in a water-mediated hydrogen bond with its β_2His143 counterpart (Vasquez *et al.*, 1998). All of the described interactions for β_1His143 are also observed for the symmetry-related residue β_2His143. Compared with the COHbA phosphate positions, the water molecules in 1aj9 that mediate hydrogen bonds between β_1His143 and β_2His143 are roughly 3.5 Å further down the central water cavity.

None of the COHbA and 1aj9 interactions involving the four histidine residues and the phosphate or water molecules, respectively, are observed in the R-state 1hh0 (Shaanan, 1983) or 2hco (Baldwin & Chothia, 1979) structures. The low resolution of 2hco precluded the addition of water and/or anionic molecules to the structure. While the overall

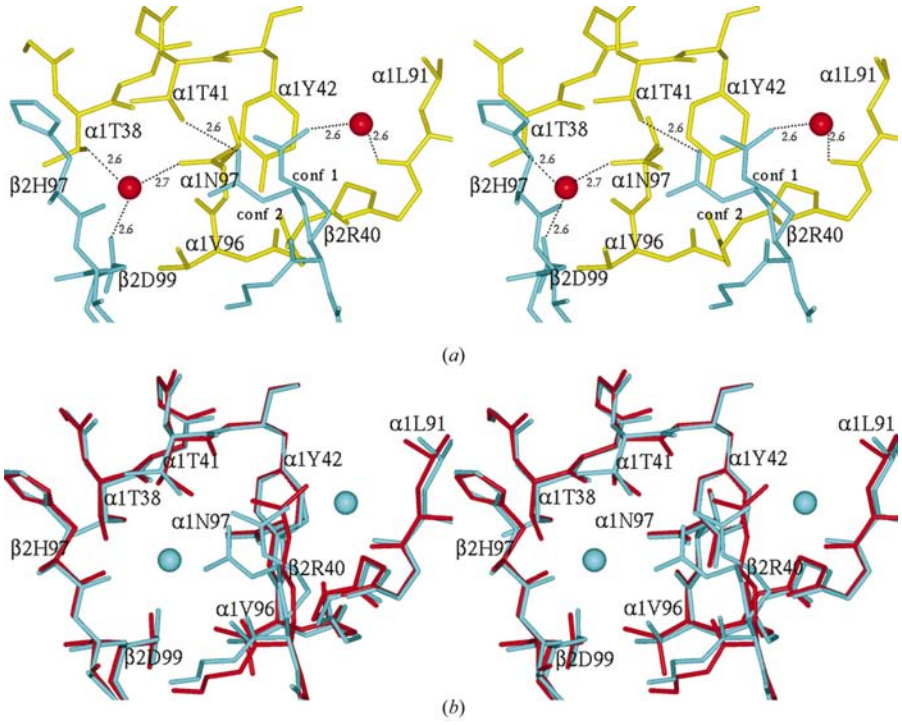

Figure 1
Stereo figure of the $\alpha_1\beta_2$ interface (*a*) of COHbA showing the reorientation of α_1Thr38 to make water-mediated interactions with β_2Asp99 and α_1Asn97 and the two alternate conformation of the β_2Arg40 side chain, (*b*) comparing COHbA (cyan) and 1aj9 (red) after superposition of the tetramers (as described in the text).

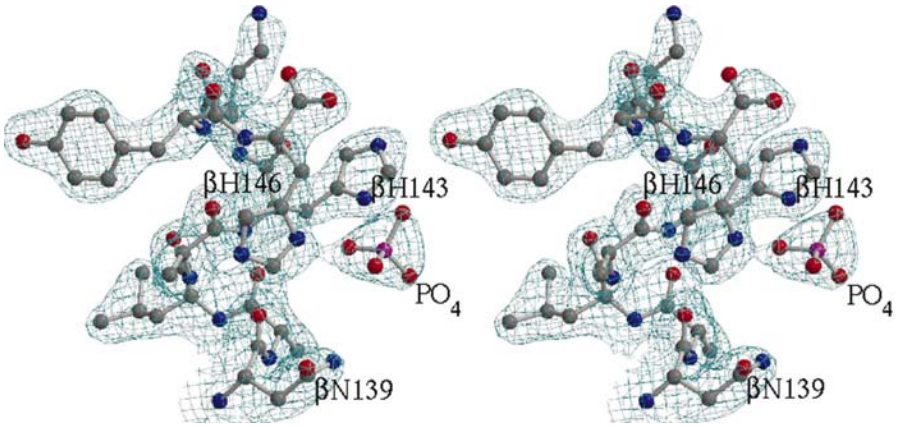

Figure 2
Stereo figure of the $2F_o - F_c$ electron-density map at the mouth of the β-subunit central water cavity showing the crystallographic phosphate and the surrounding residues. The map is contoured at 1.0σ.

backbone conformation of the β-subunit C-terminal residues of the three carbonmonoxy Hb structures and the oxyhemoglobin structure are similar, there are significant differences in the spatial arrangements of the side chains of the four histidines (βHis143 and βHis146) and the two asparagines (βAsn139). Superimposition of the C-terminal residues in the COHbA, 2hco and 1aj9 structures clearly shows that in 1aj9 and 2hco the βHis143 residues from the two β-subunits have shifted towards each other across the dyad axis (Fig. 3*b*), making the gap between these residues too narrow to accommodate the binding of a phosphate. Another difference is the position of the αAsn139 side chain in the three structures: in COHbA, the βAsn139 side chain engages in a hydrogen-bonding interaction with the phosphate; however, in 2hco and 1aj9 the βAsn139 side chain has oriented in the opposite direction, away from the observed phosphate position in COHbA. As shown in Fig. 3(*b*), the positions of the βHis146 side chains also differ in the three structures. Although not shown on Fig. 3, 1hh0 has βAsn139, βHis143 and βHis146 side-chain orientations that are similar to those of 1aj9 and 2hco. In addition, 2hco shows a slightly larger cleft between the two βHis143 residues (compared with that of 1aj9) and could potentially bind to one phosphate conformer.

Our initial experiment involved the structure determination of COHbA, which crystallized at pH 6.4, and it was surmised that the binding of the phosphate at the C-terminus was probably a consequence of the lower pH of the crystallization conditions. This prompted us to examine CO-liganded structures at different crystallization pH levels. Subsequently, the crystallization and structural solution of two new liganded COHb at pH levels of 7.1 (2.2 Å) and 5.4 (2.25 Å) were performed. Surprisingly, these two structures, like COHbA, also possessed a phosphate molecule bound close to the twofold axis. However, there were several differences. While the two phosphate conformers were well defined in the COHbA structure, with a minimum distance of 2.5 Å between the two closest atoms of the conformers, the phosphate molecule found in the other CO-liganded structures at pH 7.1 and 5.4 had lower occupancy. Moreover, the two phosphate conformers in the two new structures were also much closer to one another; a distance of 1.8 Å was measured between the two closest atoms in the bound phosphates. In addition, the interaction involving βAsn139 was lost (as this residue was oriented away from the phosphate), while interactions with His143 and His146 were significantly weakened. This was reflected in higher *B* factors for the C-terminal residues of these two structures. Like COHbA, a similar loss of hydrogen bonding between β_2His97 O and α_1Thr38 OG1 in both structures was also observed, with α_1Thr38 reorienting to form water-mediated interactions with β_2Asp99 OD1 and α_1Asn97 ND2. However, in both of the new liganded structures β_2Arg40 was in only one conformation, corresponding to the β_2Arg40 position in 1aj9, and was engaged in a normal diagnostic R-state hydrogen-bonding interaction with α_1Thr41. Based on these results, it seems that the side chains of the β-subunit C-terminal residues in the R-state structures can easily rotate. This would account for the slight differences in their positions in each of the analyzed CO-liganded structures described in this study.

No significant differences between the heme environments of COHbA and 1aj9 were observed. One exception, however, involved the Fe—C—O angle. In COHbA, the Fe—C—O angles were restrained during the refinement, resulting in angles of 177° in the α-heme and 173° in the β-heme. The corresponding angles in 1aj9 are 125 and 162°, respectively, and were not restrained during the refinement (Vasquez *et al.*, 1998).

3.3. Structural comparison with T-state Hb

The structures of COHbA and the T-state deoxyhemoglobin–2,3-DPG complex (PDB code 1b86; Richard *et al.*, 1993) were compared by superimposing the two tetramers on atom positions that define the dyad axis of the two structures. This was achieved by placing an imaginary atom at the center of the tetramer on the dyad axis of each Hb structure. Atoms were then placed at specific distances from the central atom position along the two directions of the dyad axis. The two structures were then superimposed on corresponding atom positions along this axis.

Superposition of R-state COHbA and T-state 1b86 on the dyad axis indicated that the two phosphate conformers in COHbA overlapped the position occupied by 2,3-DPG in 1b86 (Fig. 4). However, rearrangements of the β-cleft residues during the allosteric transition resulted in several differences in the interactions associated with these small molecules and protein residues in the two structures. In COHbA, the phosphate molecule interacts with residues βAsn139, βHis143 and βHis146, while in 1b86, 2,3-DPG is observed to interact with residues βHis2 and βLys82 (Richard *et al.*, 1993). In addition, a previous study by Arnone (1972) found that DPG engages in contacts with βVal1, βLys82 and β143, while a study by Bunn & Briehl (1970) found that four residues, βVal1, βHis2, βLys82 and β143, are critical for 2,3-DPG binding. 2,3-DPG is known to bind almost exclusively to the larger β-cleft of the T-state structure, leading to stabilization of the T state relative to the R state. As indicated by Baldwin (1975), the narrowing of the β-cleft in R-state Hb reduces the binding constant of 2,3-DPG by a factor of more than 100 compared with the binding constant of T-state Hb. Interestingly, the cleft that allows phosphate binding in COHbA may reveal a glimpse at the 2,3-DPG binding site as the β-cleft widens during the transition from the R to the T state.

4. Discussion

The $\alpha_1\beta_2$ (and corresponding $\alpha_2\beta_1$) interface of the Hb tetramer is an important structural feature controlling the allosteric transition between any of the three quaternary states: R→T, R2→T and R→R2. During the allosteric transition, a 14° rotation of the $\alpha_1\beta_1$ dimer relative to the $\alpha_2\beta_2$ dimer leads to the formation of the T state from the R state. Furthermore, the R→R2 and R2→T transitions also result in rotations between the two dimers of approximately 12 and 22°,

respectively. Baldwin & Chothia (1979) were the first to characterize the $\alpha_1\beta_2$ dimer interface as consisting of a 'switch' region (interface between α_1C helix and β_2FG corner), a 'flexible joint' region (interface between α_1FG corner and β_2C helix) and an 'intermediate' region (interfaces between α_1C and β_2C helices and α_1FG and β_2FG corners). During the R→T transition, the interactions between β_2His97 O and α_1Thr38 OG1 and β_2Arg40 NH1 and α_1Thr41 O, which are located in the switch and intermediate regions, respectively, are completely lost. During the transition from the R to the R2 state, the hydrogen bond between β_2His97 and α_1Thr38 is also lost and the hydrogen bond between α_1Thr41 and β_2Arg40 is significantly weakened. Therefore, these two hydrogen bonds appear to be important for stabilizing the R state relative to the T or R2 states. The apparent weakening or loss of these two hydrogen bonds at the $\alpha_1\beta_2$ ($\alpha_2\beta_1$) interface in the newly determined R-state COHbA structure could affect the stability of this structure, which may represent a very subtle but real gradation in the transition process from the R to the T state.

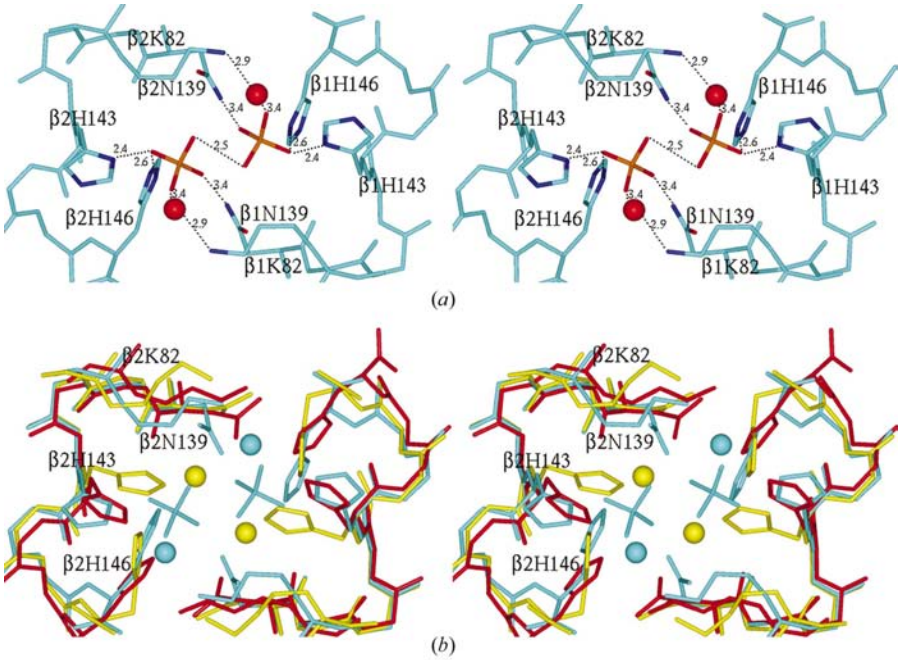

Figure 3
Stereo figure of the β-subunit water cavity (*a*) of COHbA showing the network of water- and phosphate-mediated hydrogen-bond interactions that connect β_2Lys82, β_2Asn139, β_1His143 and β_1His146 to each other and to their symmetry-related counterparts, (*b*) comparing the phosphate binding site of COHbA (cyan) with 1aj9 (yellow) and 2hco (red) after superposition of the tetramers (as described in the text).

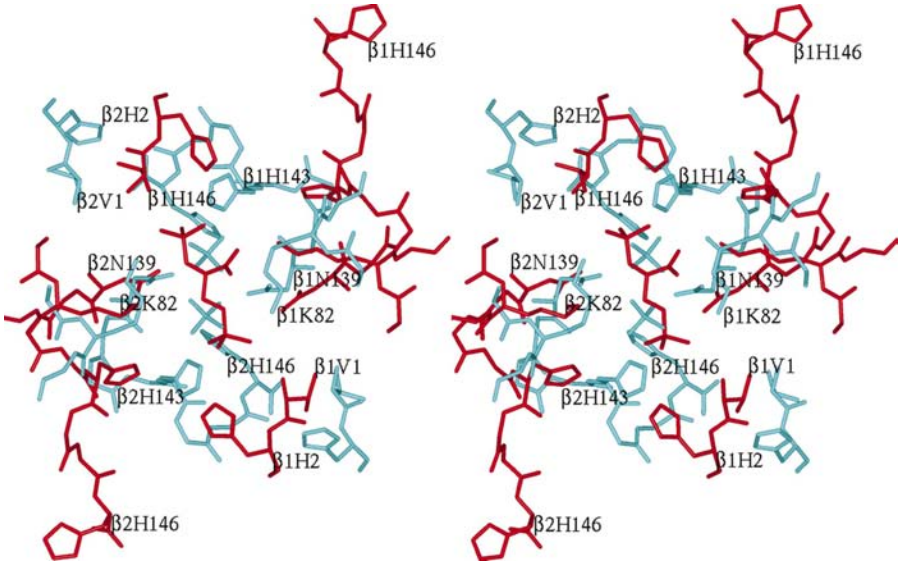

Figure 4
Stereo figure of the β-subunit water cavity comparing the phosphate binding site of COHbA (cyan) with the 2,3-DPG binding site of 1b86 (red) after superposition of the two structures on the dyad axes (as described in the text).

The most intriguing difference between the COHbA and 1aj9 structures is the presence of a phosphate molecule at the site where 2,3-DPG binds to T-state Hb. Compared with the classical R-state structure of Hb, the three new CO-liganded Hb structures, obtained at pH levels of 5.4, 6.4 and 7.1, display a weakening or loss of hydrogen-bonding interactions at the $\alpha_1\beta_2$ interface. Interestingly, COHbA (pH 6.4), which has the most tightly bound phosphate molecule at the C-terminus, displays the greatest loss in hydrogen-bond stabilization of the $\alpha_1\beta_2$ interface compared with the other two CO-liganded structures obtained at pH 7.1 and 5.4. In contrast, 1aj9 and other R-state human Hbs that lack this phosphate molecule at the C-terminus maintain the key hydrogen bonds that stabilize the R state. These observations suggest a possible correlation between the bound phosphate and the observed tertiary structural changes observed at the $\alpha_1\beta_2$ ($\alpha_2\beta_1$) interface in the CO-liganded structures described in this manuscript. It is plausible to assume that the cryoconditions (100 K) under which the data sets for the COHbA were collected are responsible for the observed binding of the phosphate. By freezing the crystals (for comparison, other R-state Hb structures were determined at either 273 K or room temperature), it is hypothesized that the bound phosphate is stabilized in its Hb binding site.

The alkaline Bohr effect, which explains the preferential uptake of protons by the T state and the release of the protons in the R state, plays a significant role in the allosteric regulation

of Hb (Perutz, 1970). About 40% of the Bohr effect (Kilmartin *et al.*, 1978) arises as a result of the salt-bridge interaction between βHis146 and βAsp126 in the T state, which leads to the uptake of a proton by βHis146. In contrast, the R state shows no such salt-bridge interaction between these two residues, which leads to a lowering of the imidazole pK_a from 8.0 in deoxygenated Hb to 7.1 in liganded Hb (Kilmartin *et al.*, 1973). As a result, there is the release of a proton by R-state Hb under physiological conditions, leading to an increase in its oxygen affinity. It is plausible to assume that the binding of the phosphate in COHbA is accompanied by protonation of the βHis146 imidazole. This would undoubtedly destabilize the R state and shift the allosteric equilibrium towards the T state, leading to the observed disruption of the two key hydrogen bonds that stabilize the R state. In effect, the bound phosphate molecule may facilitate the observed crystallographic snapshot of the allosteric transition reported in this study. Interestingly, in the structure of human carbonmonoxy β4 Hb (CO-β4), which displays some T-state characteristics, two phosphate molecules are also observed to bind at the phosphate binding site observed in this study and similarly overlap the T-state 2,3-DPG binding site (Arnone, 1972).

We gratefully acknowledge research support from NIH to MKS (grant HL04367) and DJA (grant HL32793).

References

Arnone, A. (1972). *Nature (London)*, **237**, 146–149.
Baldwin, J. & Chothia, C. (1979). *J. Mol. Biol.* **129**, 175–220.
Baldwin, J. M. (1975). *Prog. Biophys. Mol. Biol.* **29**, 225–320.
Brünger, A. T. (1992). *Nature (London)*, **35**, 422–475.
Brünger, A. T., Adams, P. D., Clore, G. M., DeLano, W. L., Gros, P., Grosse-Kunstleve, R. W., Jiang, J.-S., Kuszewski, J., Nilges, M., Pannu, N. S., Read, R. J., Rice, L. M., Simonson, T. & Warren, G. L. (1998). *Acta Cryst.* D**54**, 905–921.
Bunn, H. F. & Briehl, R. W. (1970). *J. Clin. Invest.* **49**, 1088–1095.
Cambillau, C. & Horjales, E. (1987). *J. Mol. Graph.* **5**, 174–177.
Doyle, M. L., Lew, G., Turner, G. J., Rucknagel, D. & Ackers, G. K. (1992). *Proteins Struct. Funct. Genet.* **14** 351–362.
Janin, J. & Wodak, S. J. (1993). *Proteins*, **15**, 1–4.
Katz, D. S., White, S. P., Huang, W., Kumar, R. & Christianson, D. W. (1994). *J. Mol. Biol.* **244**, 541–553.
Kilmartin, J. V., Breen, J. J., Roberts, G. C. & Ho, C. (1973). *Proc. Natl Acad. Sci. USA*, **4**, 1246–1249.
Kilmartin, J. V., Imai, K., Jones, R. T., Faruqui, A. R., Fogg, J. & Baldwin, J. M. (1978). *Biochim. Biophys. Acta.* **534**, 15–25.
Ladner, R. C., Heidner, E. J. & Perutz, M. F. (1977). *J. Mol. Biol.* **114**, 385–414.
Laskowski, R. A., Macarthur, M. W., Moss, D. S. & Thornton, J. M. (1993). *J. Appl. Cryst.* **26**, 283–291.
Monod, J., Wyman, J. & Changeux, J.-P. (1965). *J. Mol. Biol.* **12**, 88–118.
Perutz, M. F. (1968). *J. Cryst. Growth*, **2**, 54–56.
Perutz, M. F. (1970). *Nature (London)*, **228**, 726–734.
Perutz, M. F. (1972). *Nature (London)*, **237**, 459–499.
Richard, V., Dodson, G. G. & Mauguen, Y. (1993). *J. Mol. Biol.* **233**, 270–274.
Safo, M. K. & Abraham, D. J. (2001). *Protein Sci.* **10**, 1091–1099.
Schumacher, M. A., Zheleznova, E. E., Poundstone, K. S., Kluger, R., Jones, R. T. & Brennan, R. G. (1997). *Proc. Natl Acad. Sci. USA*, **94**, 7841–7844.
Shaanan, B. (1983). *J. Mol. Biol.* **171**, 31–59.
Silva, M. M., Rogers, P. H. & Arnone, A. (1992). *J. Biol. Chem.* **267**, 17248–17256.
Smith, F. R., Lattman, E. E. & Carter, C. W. Jr (1991). *Proteins*, **10**, 81–91.
Smith, F. R. & Simmons, K. C. (1994). *Proteins*, **18**, 295–300.
Srinivasan, R. & Rose, G. (1994). *Proc. Natl Acad. Sci. USA*, **91**, 11113–11117.
Vasquez, G. B., Ji, X., Fronticelli, C. & Gilliland, G. L. (1998). *Acta Cryst.* D**54**, 355–366.